Magnetoconductivity of a metal with a closed Fermi surface reconstructed by a biaxial density wave

A. M. Kadigrobov [1,2,*] B. Keran,[2] and D. Radić [2,†]

[1]*Theoretische Physik III, Ruhr-Universitaet Bochum, D-44801 Bochum, Germany*

[2]*Department of Physics, Faculty of Science, University of Zagreb, 10000 Zagreb, Croatia*

(Received 12 August 2021; accepted 13 October 2021; published 25 October 2021)

We investigate quantum dynamics and kinetics of a 2D conductor with a closed Fermi surface reconstructed by a biaxial density wave, in which electrons move along a two-dimensional periodic net of semiclassical trajectories coupled by the magnetic breakdown tunneling under a strong magnetic field. We derive a quasiparticle dispersion law and magnetoconductivity tensor. The quasiparticle spectrum is found to be the alternating series of two-dimensional magnetic energy bands with gaps between them. The longitudinal magnetoconductivity shows giant oscillations with change of magnetic field, while the Hall coefficient changes sign and is absent in a wide range of the magnetic fields in between. Preliminary estimations show that the suggested magnetoconductivity mechanism may be the origin of such behavior of the Hall coefficient versus magnetic field, as observed in experiments in materials with analogous topology of the Fermi surface, such as the high-T_c superconducting cuprates.

DOI: 10.1103/PhysRevB.104.155143

I. INTRODUCTION

Systems with charge carriers interacting with phonons or other excitations in one- and two-dimensional (1D and 2D) geometry are often found to be unstable with respect to spontaneous arising of a periodic modulation of charge or spin density, which is usually called the density wave (DW) [1]. Such periodic ordering is stabilized whenever the decrease of the electronic band energy, which occurs due to the reconstruction of the Fermi surface (FS), overcomes the increase of the crystal energy caused by the crystal lattice modulation or electron-electron interactions. In 1D conductors, such modulation opens a gap in an electron spectrum at the Fermi energy, thus decreasing the electron band energy, constituting the well-known Peierls instability [2]. The DW instability is most commonly encountered in 2D conductors with highly anisotropic open FSs, such that entire or a great part of its contour can be mapped onto each other by a single wave vector. It is known as the nesting mechanism of the DW stabilization [1,3,4]. DWs have also been observed in conductors with closed and convex FSs, such as high-T_c superconducting cuprates [5] or intercalated graphite compounds [6], the DW instability of which cannot be explained within the above-mentioned nesting mechanism. A possible explanation of this phenomenon was recently suggested in our papers [7–9]. This mechanism is based on the topological reconstruction of the initially closed FS into an open one, the latter being composed of the initial FSs which slightly overlap (nearly touch) one another with (pseudo) gap opening around the touching region.

Of particular interest are not only the DW properties but also a response of such system to external fields, temperature, or currents. Conductance and its dependence on magnetic field are of great importance both for fundamental science and applications. Such phenomena as the de Haas–van Alphen, or Shubnikov-de Haas oscillations, as well as the Hall effect, provide a powerful tool for the investigations of new characteristics of the material imposed by the DW such as, for example, the quasiparticle FS reconstructed by the DW. Change of signs of the Hall coefficient [10] and its zero-value in a wide interval of magnetic field [11], observed in experiments on high-T_c superconducting cuprates, are particularly intriguing.

In this paper, we investigate dynamics and kinetics of quasiparticles in a 2D conductor, with a DW ordering, under a strong magnetic field perpendicular to the sample. We consider the case of biaxial DW (so-called checkerboard pattern), characterized with two perpendicular wave vectors of the same size, which brings the initial closed FSs into a 2D net of FSs very slightly overlapping (nearly touching) one another. By lifting the energy degeneracy and opening the gap around the points of contact, the FS is transformed into a periodic set of closed diamond-shaped pockets, which are close to each other at the edges of the new Brillouin zones in the extended zone scheme [12] (see Fig. 1).

Under a strong magnetic field, quasiparticles move along the semiclassical trajectories undergoing magnetic breakdown (MB) in the small gapped area around the touching points (MB region shown shaded/dotted in Fig. 1) with the MB probability [13–16]

$$|t|^2 \approx 1 - \exp\left(-\frac{\Delta^2}{(\hbar\omega_H)^{4/3}\varepsilon_F^{2/3}}\right) \tag{1}$$

to scatter and continue motion along the diamond-shaped orbit, and probability $|r|^2 = 1 - |t|^2$ to tunnel through the semiclassically forbidden regions and move along the circular

*anatolykadigrobov@gmail.com

†dradic@phy.hr

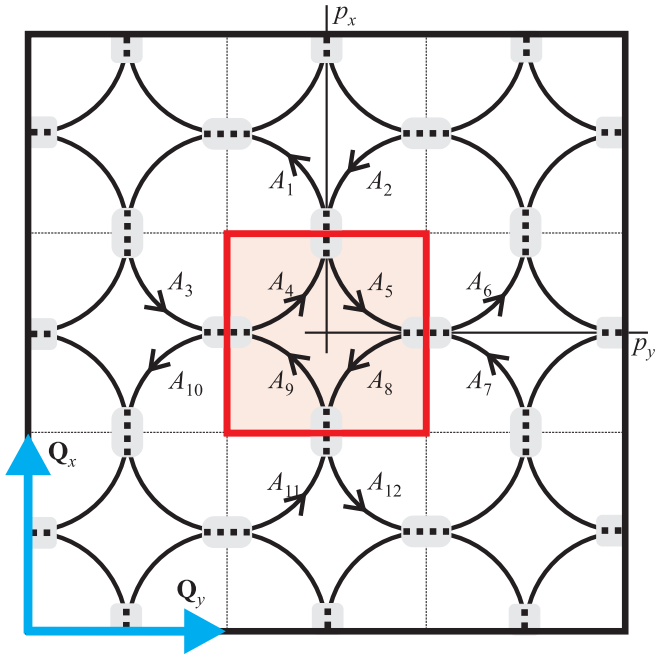

FIG. 1. The Fermi surface (extended zone scheme) of investigation of a 2D conductor reconstructed by the biaxial density wave (characterized by wave vectors $\mathbf{Q}_x$ and $\mathbf{Q}_y$ in x and y directions). Initially circular contours (electronlike) are transformed into a set of diamondlike contours (holelike) separated by gaps (shaded gray) in small areas at the Brillouin zone boundary (red square). Under the magnetic field perpendicular to the plane, quasiparticles move in the momentum space (p_x, p_y) along the semiclassical trajectories (arrows) undergoing the MB scattering at the gapped areas (dotted paths). $A_1 - A_{12}$ are constants related to the semiclassical wave functions on the corresponding trajectories in the 2D MB net.

orbit. There $\omega_H = eH/m$ is the cyclotron frequency, H is the magnetic field, e is the electron charge (absolute value), m is the electron effective mass, ε_F is the Fermi energy and Δ is the gap in the quasiparticle energy spectrum. This equation for the MB probability differs from the well-known Blount formula [17–19] $|t|^2 = 1 - \exp\left(-\Delta^2/(\hbar\omega_H|v_x^{(0)}v_y^{(0)}|)\right)$, where $v_x^{(0)}$ and $v_y^{(0)}$ are the velocity projections at the MB point between trajectories crossing each other before opening of the gap. This difference appears because one of the velocity projections in the Blount probability would be equal to zero if the MB takes place between the trajectories touching each other as in the present case.

We calculate spectrum of quasiparticles moving in such a 2D MB net under magnetic field [20], satisfying the condition that Φ/Φ_0 is a rational number, where Φ is the magnetic flux threading the unit cell and $\Phi_0 = h/e$ is the magnetic flux quantum (h is the Planck's constant). This condition, appearing in our problem, is analogous to the one from the well-known works of Zak [21] and Hofstadter [22], coming from the requirement that the wave function must be uniquely defined, i.e., from the required commensurability of the new periodicity imposed by the magnetic field with the periodicity of the underlying lattice imposed by the crystal potential or the DW. Our analytical calculations show that the quasiparticle spectrum in such a system is a serial of alternating 2D energy bands with gaps between them.

Using this spectrum, we calculate the 2D magnetoconductivity tensor σ_{ij}, $i, j \in \{x, y\}$ and find that the diagonal conductivities σ_{xx} and σ_{yy} perform giant oscillations with a change of magnetic field in the whole interval of H in which the MB is distinct, i.e., $|t||r| \sim 1$. It is particularly remarkable that $\sigma_{xy} = 0$ and hence the Hall coefficient $R_H = 0$ everywhere inside this wide interval of magnetic field.

We also show that the conventional magnetoconductivity tensor for closed orbits [23] restores in the limits of relatively weak, i.e., $|r(H)| \ll 1$, and relatively strong magnetic fields, i.e., $|t(H)| \ll 1$, in which broadening of the Landau levels by the MB is much smaller than the energy uncertainty caused by the quasiparticle-impurity scattering characterized by the scattering frequency ν_0. The Hall coefficient has opposite signs in these two limits (and vanishes between them).

The paper is organized as follows: In Sec. II, we consider dynamics of quasiparticles moving in the 2D periodic net of semiclassical trajectories coupled by the MB, finding the quasiparticle wave functions and dispersion law in the momentum representation. In Sec. III, we calculate the magnetoconductivity tensor. Section IV contains the concluding remarks. In the Appendixes, we show mathematical details related to the calculation of the above-mentioned quantities.

II. DYNAMICS OF QUASIPARTICLES IN A TWO-DIMENSIONAL NET OF ORBITS UNDER MAGNETIC BREAKDOWN CONDITIONS

Recently, we have shown that a homogeneous state of electrons in 2D conductors with closed FSs may be unstable with respect to spontaneous arising of a uniaxial DW in the system [7–9]. In this paper, we consider a 2D conductor, with initial quasiparticle spectrum $\varepsilon(p_x, p_y)$ and momentum $\mathbf{p} = (p_x, p_y)$, and closed FS determined by $\varepsilon(p_x, p_y) = \varepsilon_F$, in which the structural instability is caused by a biaxial DW characterized by two perpendicular wave vectors $\mathbf{Q}_x$ and $\mathbf{Q}_y$ in x and y directions, respectively. We consider the case which results in a reconstruction of the initial closed FSs into a 2D periodic set of (new) FSs which are close to each other at the edges of the (new) Brillouin zones in the extended zone scheme as shown in Fig. 1. Under a strong magnetic field $\varepsilon_F/\hbar \gg \omega_H \gg \nu_0$, the quasiparticle moves in the momentum space along the semiclassical trajectories at energy $\varepsilon(p_x, p_y) = \varepsilon$ between the MB regions, undergoing the MB scatterings at them.

The semiclassical motion of the quasiparticle in the momentum space along the semiclassical trajectories between the MB points is described by the Lifshitz-Onsager Hamiltonian [24,25]. Choosing the Landau gauge for the vector potential, $\mathbf{A} = (-Hy, 0, 0)$, one writes the Schrödinger equation in the momentum representation for quasiparticles moving between the MB points,

$$\varepsilon_\alpha\left(P_x + ib_H^2\frac{d}{dp_y}, p_y\right)G_\alpha(p_y) = \varepsilon G_\alpha(p_y), \tag{2}$$

where $\varepsilon_\alpha(p_x, p_y)$ is the initial quasiparticle dispersion law which is shifted to the position corresponding to the trajectory α (the index α denotes the quasiparticle trajectory between

two neighboring MB points—see Fig. 1) and P_x is the conserved generalized momentum projection. Here $b_H^2 = e\hbar H$ is the elementary magnetic area in the momentum space, related to the magnetic (cyclotron) energy as $\hbar\omega_H = b_H^2/m$.

The semiclassical solution of Eq. (2) is

$$G_\alpha(p_y) = \frac{A_\alpha}{\sqrt{v_x^\alpha}} e^{i(P_x p_y/b_H^2)} e^{iS_\alpha(p_y)/b_H^2}, \tag{3}$$

where A_α are constants which are determined by matching of the wave functions. The velocity

$$v_x^\alpha(p_y) = \frac{\partial\varepsilon_\alpha(\mathbf{p})}{\partial p_x}\Big|_{p_x = dS_\alpha/dp_y} \tag{4}$$

is determined by the momentum space area (phase)

$$S_\alpha(p_y) = \int_0^{p_y} p_x^\alpha(\varepsilon, p_y')dp_y', \tag{5}$$

where the integrated function $p_x^\alpha(\varepsilon, p_y')$ is found from the algebraic equation

$$\varepsilon_\alpha(p_x, p_y') = \varepsilon. \tag{6}$$

The beginning of the integration $p_y = 0$ is chosen to be a starting point of the quasiparticle motion along the trajectory α (the arrows in Fig. 1 show the direction of quasiparticle motion).

Inside the small areas (shaded and marked by thick dots in the figure), in which the semiclassical trajectories closely approach each other, the quasiparticle undergoes a quantum tunneling between them (so-called magnetic breakdown [17,26]—MB). At the MB points, the outgoing and incoming wave functions are related by the 2×2 unitary matrix—the MB matrix,

$$\hat{\tau} = e^{i\chi}\begin{pmatrix} t & r \\ -r^\star & t^\star \end{pmatrix}, \tag{7}$$

where t and r are the complex amplitudes of the beforementioned probabilities for quasiparticle motion along the diamond-shaped or circular orbit, respectively, after scattering in the MB region, fulfilling the condition $|t|^2 + |r|^2 = 1$, χ is the real phase. All four independent parameters of the MB matrix depend on magnetic field [13–16]. Therefore, in the momentum representation, the wave function of the quasiparticle moving along the 2D net under magnetic field takes the form

$$G(p_x, p_y) = e^{i(P_x p_y/b_H^2)} \sum_\alpha \frac{A_\alpha}{\sqrt{v_x^\alpha}} e^{iS_\alpha(p_y)/b_H^2}, \tag{8}$$

where the wave functions under summation are coupled by the MB matrix Eq. (7). Note that the dependence of the wave function $G(p_x, p_y)$ on p_x is implicitly present in the A_α and the position of the trajectory α.

Matching all the semiclassical wave functions, Eq. (3), related to the first Brillouin zone with the MB matrix, one finds a set of eight algebraic equations for coefficients A_α:

$$\begin{pmatrix} A_1 \\ A_5 \end{pmatrix} = e^{i\chi}\begin{pmatrix} t & r \\ -r^\star & t^\star \end{pmatrix}\begin{pmatrix} A_2 e^{i\Theta_2} \\ A_4 e^{i\Theta_4} \end{pmatrix},$$

$$\begin{pmatrix} A_4 \\ A_{10} \end{pmatrix} = e^{i\chi}\begin{pmatrix} t & r \\ -r^\star & t^\star \end{pmatrix}\begin{pmatrix} A_9 e^{i\Theta_9} \\ A_3 e^{i\Theta_3} \end{pmatrix},$$

$$\begin{pmatrix} A_9 \\ A_{12} \end{pmatrix} = e^{i\chi}\begin{pmatrix} t & r \\ -r^\star & t^\star \end{pmatrix}\begin{pmatrix} A_8 e^{i\Theta_8} \\ A_{11} e^{i\Theta_{11}} \end{pmatrix},$$

$$\begin{pmatrix} A_6 \\ A_8 \end{pmatrix} = e^{i\chi}\begin{pmatrix} t & r \\ -r^\star & t^\star \end{pmatrix}\begin{pmatrix} A_7 e^{i\Theta_7} \\ A_5 e^{i\Theta_5} \end{pmatrix}, \tag{9}$$

where

$$\Theta_\alpha = \frac{S_\alpha(p_\alpha^e)}{b_H^2} \tag{10}$$

are the phase gains obtained by the wave function Eq. (3) during the quasiparticle motion from the beginning to the end of the trajectory α. There, p_α^e is the p_y coordinate of the trajectory ending point with respect to the direction of motion.

As one sees from the Eq. (8), the sought wave function $G(p_x, p_y)$ is the proper function of the translation operator $\hat{T}_y = e^{b_y\partial/\partial p_y}$, i.e.,

$$\hat{T}_y G(p_x, p_y) = e^{i(P_x b_y/b_H^2)} G(p_x, p_y) \tag{11}$$

for any value of magnetic field, where b_y is the (reciprocal) lattice constant in the p_y direction of the reciprocal (momentum) space after reconstruction. The eigenvalue is characterized by the proper generalized momentum P_x. The 2D net of the MB-coupled trajectories is geometrically periodic (see Fig. 1) in both p_x and p_y directions and, hence, one may assume that the quasiparticle wave function $G(p_x, p_y)$ is a proper function not only of the translation operator $\hat{T}_y$, but also of $\hat{T}_x = e^{b_x\partial/\partial p_x}$ with the proper generalized momentum P_y, i.e.,

$$\hat{T}_x G(p_x, p_y) = e^{i(P_y b_x/b_H^2)} G(p_x, p_y), \tag{12}$$

where b_x is the analogous reciprocal lattice constant in p_x direction. In this case, as it follows from Eqs. (3), (11), (12), and Fig. 1, constants A_α are additionally coupled by the conditions

$$\begin{aligned} A_2 &= A_8 e^{iP_y b_x/b_H^2}; \quad A_{11} = A_4 e^{-iP_y b_x/b_H^2}, \\ A_1 &= A_9 e^{iP_y b_x/b_H^2}; \quad A_{12} = A_5 e^{-iP_y b_x/b_H^2}, \\ A_6 &= A_4 e^{iP_x b_y/b_H^2}; \quad A_3 = A_5 e^{-iP_x b_y/b_H^2}, \\ A_7 &= A_9 e^{iP_x b_y/b_H^2}; \quad A_{10} = A_8 e^{-iP_x b_y/b_H^2}, \end{aligned} \tag{13}$$

where we note the phase factors determined by the conserved generalized momenta P_x and P_y. As a result, we have 16 equations, Eqs. (9) and (13) for 12 unknown coefficients A_α. Since the number of equations is larger than the number of unknowns, the system is overdetermined and, hence, cannot be solved as such.

However, as one can see from the definition of the phase gains Eq. (10) and Fig. 1, there are the following relations between phases:

$$\begin{aligned} \Theta_2 &= \Theta_8 + \frac{b_x b_y}{2b_H^2}; \quad \Theta_3 = \Theta_5, \\ \Theta_{11} &= \Theta_4 - \frac{b_x b_y}{2b_H^2}; \quad \Theta_7 = \Theta_9. \end{aligned} \tag{14}$$

If magnetic field is chosen to satisfy condition

$$\frac{b_x b_y}{2b_H^2} = \pi\frac{\Phi_0}{a_x a_y H} = 2\pi l, \tag{15}$$

where l is an integer (in our case $l \gg 1$), a_x and a_y are reconstructed lattice constants in the real space, and $\Phi = a_x a_y H$ is thus the magnetic flux piercing the unit cell, only four equations from the set of eight equations Eqs. (9) are independent, hence making the total system of equations solvable [27]. As already mentioned in the Introduction, this condition is consistent with works of Zak and Hofstadter [21,22], so we call it Zak's condition in this paper. Inserting Eq. (14) into Eqs. (9), one easily finds that the first four and last four equations are identical. Therefore, for the magnetic fields satisfying Zak's condition Eq. (15), the set of equations Eqs. (9) reduces to the system of four equations for four unknowns, i.e.,

$$\begin{aligned} &+rA_4 e^{i(\Theta_{11}-K_y)} + tA_8 e^{i\Theta_8} - A_9 e^{-i\chi} = 0,\\ &-t^\star A_5 e^{i\Theta_5} + A_8 e^{-i\chi} + r^\star A_9 e^{i(\Theta_7+K_x)} = 0,\\ &-t^\star A_4 e^{i\Theta_4} + A_5 e^{-i\chi} + r^\star A_8 e^{i(\Theta_2+K_y)} = 0,\\ &-A_4 e^{-i\chi} + rA_5 e^{i(\Theta_3-K_x)} + tA_9 e^{i(\Theta_9)} = 0, \end{aligned} \tag{16}$$

that determine the quasiparticle wave function Eq. (8) and the quasiparticle spectrum.

Calculating the determinant of the above set of homogeneous algebraic equations

$$\begin{aligned} D(\varepsilon, \mathbf{P}) = \sin&\left[\frac{S_\diamond(\varepsilon)}{2b_H^2} + 2\chi\right]\\ &+ |t||r|\left\{\sin\left[\frac{b_y P_x}{b_H^2} + \mu - \eta\right]\right.\\ &\left.+ \sin\left[\frac{b_x P_y}{b_H^2} - \mu - \eta\right]\right\}, \end{aligned} \tag{17}$$

where $\mathbf{P} = (P_x, P_y)$, one finds the dispersion equation for quasiparticles moving in the 2D lattice under magnetic field:

$$D(\varepsilon, \mathbf{P}) = 0. \tag{18}$$

Here $S_\diamond$ is the area of the diamond-shaped trajectory in Fig. 1, related to the circular-shaped one $S_\circ = 2\pi m\varepsilon$, by the relation $S_\diamond(\varepsilon) = b_x b_y - S_\circ = b_x b_y - 2\pi m\varepsilon$, while μ and η are phases of the probability amplitudes t and r, respectively.

The quasiparticle spectrum found from Eq. (18) reads

$$\begin{aligned} \varepsilon_s(P_x, P_y) = \hbar\omega_H\Bigg\{&s + \frac{2\chi}{\pi}\\ &+ \frac{(-1)^s}{\pi}\arcsin\left[|tr|\left(\sin\left(\frac{b_y P_x}{b_H^2} + \mu - \eta\right)\right.\right.\\ &\left.\left.+ \sin\left(\frac{b_x P_y}{b_H^2} - \mu - \eta\right)\right)\right]\Bigg\}, \end{aligned} \tag{19}$$

where $s = 0, 1, 2, \ldots$ is the new band index and is shown in Fig. 2. One can see from Eq. (19) and Figs. 2(a) and 2(b) that the spectrum consists of the periodic series of alternating (magnetic) energy bands of the width

$$W(H) = \frac{2}{\pi}\arcsin[2|t(H)r(H)|]\hbar\omega_H \tag{20}$$

and gaps of the width $\hbar\omega_H - W$ between them. The function $|t(H)r(H)|$ takes values between 0 and 1/2 [see Fig. 2(c)]. In the limit $|t(H)| = 0$ or $|r(H)| = 0$, we have Landau levels due to the Landau quantization of circular or diamond-shaped orbits, respectively. In the intermediate regime, starting with $|t| \ll 1$ in one and $|r| \ll 1$ in another mentioned limit, the Landau levels are broadened into magnetic energy bands due to the MB, with gaps in between. In the limit $|tr| = 1/2$, the gap closes in the Γ and M points in the Brillouin zone, with approximately linear dispersion around them [see Fig. 2(b)]. Spectrum also exhibits rapid oscillations with respect to magnetic field [see Fig. 2(d)] with period determined by the area of the pocket encircled by the semiclassical trajectory.

It is worth noticing that the quasiparticle group velocity is of the order of the Fermi velocity v_F in spite of the fact that the bandwidth is very narrow, i.e., $\mathbf{v} = \partial\varepsilon_s/\partial\mathbf{P} \sim |tr|b/m \sim 10^6 m/s$ for $|tr| \sim 1$, where, for the sake of simplicity, we assumed the cubic lattice symmetry, i.e., $b_x = b_y \equiv b$.

Also, it is important to emphasize, once more, that the spectrum Eq. (19), as well as all quantities following from it (e.g., conductivity discussed in the next section) is valid for the magnetic fields satisfying Zak's condition Eq. (15). Number l determines how many unit cells in real space host one flux quantum and, for materials with lattice constant of angström size, this number is huge, of the order of 10^4 for magnetic fields of the order of 10 T. Resolution of magnetic field, corresponding to the change of l by one, is of the order of 10^{-3}T in such systems. It is known [28] that the Zak/Hofstdater effect of flux quantization versus the underlying lattice is observable for specially engineered structures with large unit cells, very strong magnetic fields, and clean samples. It is also possible to generalize the present analysis to the periodicities in the reciprocal space involving multiple reciprocal unit cells, e.g., by using the transfer matrix or some other method, however, neither of the two above-mentioned issues are in the focus of this paper and will be discussed elsewhere.

III. KINETICS OF QUASIPARTICLES IN THE 2D NET OF SEMICLASSICAL TRAJECTORIES UNDER THE MB CONDITIONS

In this section, we consider kinetics of quasiparticles in the 2D MB net under magnetic field which satisfies Zak's condition Eq. (15). Due to the MB scattering, for which the corresponding amplitudes $|t(H)|$ and $|r(H)|$ are comparable, a 2D quasiparticle is delocalized in both directions, moving along the diamond-shaped and circular orbits as well as tunneling between them, having two conserved generalized momenta, P_x and P_y, consequently resulting in the quasiparticle dispersion equation Eq. (18). The width of the quasiparticle energy band, Eq. (20), essentially depends on the function $|t(H)r(H)|$, thus defining two characteristic limits of weak and strong magnetic field in which $|t(H)r(H)| \to 0$ [see Fig. 2(c)]. Consequently, $W \to 0$ in those limits, determining two intervals of magnetic field in which kinetics (and dynamics) of quasiparticles is qualitatively different:

1) If the bandwidth is much greater than the energy uncertainty due to scattering on impurities, i.e., $W \gg \hbar\nu_0$, the quasiparticle is delocalized and its group velocity is large in both directions, i.e., $\mathbf{v} = \partial\varepsilon_s/\partial\mathbf{P} \sim |t(H)r(H)|v_F$.

2) If the bandwidth is much smaller than the energy uncertainty due to scattering on impurities, i.e., $W \ll \hbar\nu_0$, the effective spectrum is a serial of Landau energy levels

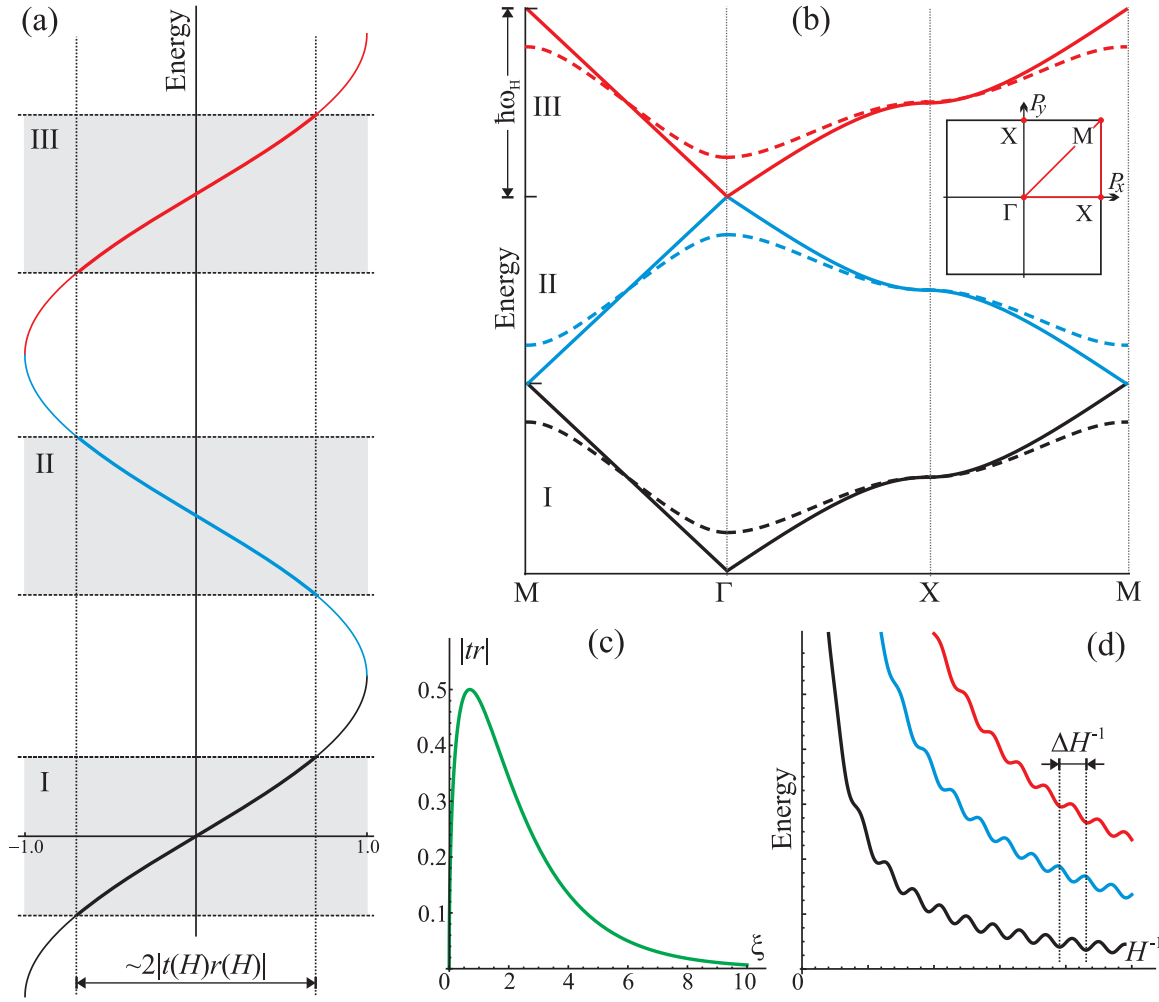

FIG. 2. Spectrum of quasiparticles: (a) Formation of the energy bands (along vertical axis, indexed by I, II, III,...) depending on argument of the arcsin function (curve) in Eq. (19) shown on the horizontal axis, which is proportional to $|t(H)r(H)|$, determining the width of the bands Eq. (20). (b) Energy dispersion in the momentum space along the lines between the characteristic points (see the inset). Width of the magnetic energy bands is maximal, i.e., $\hbar\omega_H$, for $|tr| = 1/2$ (full lines) and the gap is closed. For $|tr| < 1/2$ (dashed), the bandwidth is smaller and gaps between bands appear. (c) Function $|t(\xi)r(\xi)| = \exp[-\xi/2]\sqrt{1-\exp[-\xi]}$, where the argument $\xi \equiv \Delta^2(\hbar\omega_H)^{-4/3}\varepsilon_F^{-2/3}$ depends on magnetic field. (d) Energy spectrum taken at the Γ point depending on magnetic field exhibits rapid oscillations with period $\Delta H^{-1} \approx he/p_F^2$ with respect to the inverse magnetic field H^{-1} (p_F is the Fermi momentum determined by the area of the pocket encircled by the quasiparticle trajectory, e.g., $S_\circ \approx \pi p_F^2$). For simplicity, we set the phase $\chi = \pi/4$ in Eq. (19), valid in the limit of Landau levels.

corresponding to the quasiparticle motion along the diamond-shaped trajectory for $t(H) \to 1$ or the circular one for $r(H) \to 1$ (see Fig. 1). Therefore, in those limiting cases, the magnetoconductivity tensor is the standard one, corresponding to the closed FSs, well known from literature [23].

A. Magnetoconductivity of quasiparticles delocalized by the MB in both *x*- and *y*-direction of the 2D net

Here we assume the inequality $W \gg \hbar v_0$ and find the magnetoconductivity tensor for quasiparticles.

The linearized equation for the density matrix $\hat{\rho} = f_0(\hat{H}_0) + \hat{\rho}^{(1)}$ for quasiparticles under electric field $\mathbf{E}$ reads

$$\frac{1}{i\hbar}[\hat{H}_0, \hat{\rho}^{(1)}] + \frac{\hat{\rho}^{(1)}}{t_0} = -\frac{e\mathbf{E}}{i\hbar}[\hat{\mathbf{r}}, f_0(\hat{H}_0)]. \tag{21}$$

Here $\hat{H}_0$ is the quasiparticle effective Hamiltonian, the Schrödinger equation for which is

$$\hat{H}_0|n, \mathbf{P}\rangle = \varepsilon_n(\mathbf{P})|n, \mathbf{P}\rangle, \tag{22}$$

where the proper energy $\varepsilon_n(\mathbf{P})$ is defined by the dispersion equation Eq. (18) and the proper functions are Bloch functions, t_0 is the relaxation time (time of the mean-free path of a quasiparticle), f_0 is the Fermi distribution function, and $\hat{\rho}^{(1)}$ is the first correction to $\hat{\rho}$ with respect to linearization.

Taking matrix elements of the density matrix Eq. (21) and using the fact that both projections of velocity are finite, $v_x \neq 0$ and $v_y \neq 0$, one finds the density matrix

$$\rho^{(1)}_{\kappa\kappa'} = e\mathbf{E}\frac{i\hbar\mathbf{v}_{\kappa\kappa'}}{\varepsilon_\kappa - \varepsilon_{\kappa'} + i\hbar v_0}\frac{f_0(\varepsilon_\kappa) - f_0(\varepsilon_{\kappa'})}{\varepsilon_\kappa - \varepsilon_{\kappa'}}, \tag{23}$$

where $\kappa = (\mathbf{P}, n)$ and $\mathbf{v}_{\kappa\kappa'}$ are the the velocity matrices:

$$\mathbf{v}_{\kappa\kappa'} = \frac{\partial\varepsilon_\kappa}{\partial\mathbf{P}}\delta(\mathbf{P}-\mathbf{P}')\delta_{n,n'}. \tag{24}$$

As the quasiparticle group velocity is not zero, the main contribution to the current $\mathbf{j} = -2e\mathrm{Tr}(\hat{\mathbf{v}}\hat{\rho})$, where factor 2 accounts for the quasiparticle spin and Tr denotes the trace operation, comes from the diagonal element of the density matrix Eq. (23) and, hence, the conductivity is

$$\sigma_{ik} = -2e^2t_0\sum_n\int\frac{d\mathbf{P}}{(2\pi\hbar)^2}\frac{\partial\varepsilon_n}{\partial P_i}\frac{\partial\varepsilon_n}{\partial P_k}\frac{\partial f_0}{\partial\varepsilon}\Big|_{\varepsilon=\varepsilon_n(\mathbf{P})}, \tag{25}$$

where $i,k\in\{x,y\}$ (details of calculations are presented in Appendix A).

For calculations of various thermodynamic and kinetic coefficients of quasiparticles with complicated dispersion laws, it is convenient to use the approach developed by Slutskin [29] for electrons under the MB in which one uses the dispersion equation for calculations instead of the complicated dispersion law. Differentiating dispersion equation Eq. (18) with respect to $\mathbf{P}$, i.e., $\partial_\varepsilon D\cdot\partial_{P_i}\varepsilon + \partial_{P_i}D = 0$, one finds

$$v_i = \frac{\partial\varepsilon_n}{\partial P_i} = -\frac{\partial D(\varepsilon,\mathbf{P})/\partial P_i}{\partial D(\varepsilon,\mathbf{P})/\partial\varepsilon}, \tag{26}$$

with $D(\varepsilon,\mathbf{P}) = 0$. This expression allows to present the conductance, Eq. (25), in the sought form (see Appendix B):

$$\sigma_{ik} = -2e^2t_0\int d\varepsilon\frac{\partial f_0}{\partial\varepsilon}\int\frac{d\mathbf{P}}{(2\pi\hbar)^2}\frac{\frac{\partial D}{\partial P_i}\frac{\partial D}{\partial P_k}}{|\frac{\partial D}{\partial\varepsilon}|}\delta[D(\varepsilon,\mathbf{P})]. \tag{27}$$

Using Eq. (18), one can write Eq. (27) in the form

$$\sigma_{ik} = -2e^2t_0\frac{\bar{b}_i\bar{b}_k}{\pi mb_H^2}|tr|^2\int d\varepsilon\frac{\partial f_0/\partial\varepsilon}{|\cos\Theta_\diamond|}\int\frac{d\mathbf{P}}{(2\pi\hbar)^2} \times\cos\Theta_i\cos\Theta_k\delta[\sin\Theta_\diamond(\varepsilon)-|rt|(\sin\Theta_x+\sin\Theta_y)], \tag{28}$$

where the bar denotes the index conjugation, i.e., $\bar{b}_x = b_y$, $\bar{b}_y = b_x$, and

$$\Theta_\diamond = \frac{S_\diamond(\varepsilon)}{2b_H^2}+\chi,$$
$$\Theta_x = \frac{P_xb_y}{b_H^2}+\mu-\nu,$$
$$\Theta_y = \frac{P_yb_x}{b_H^2}-\mu-\nu. \tag{29}$$

One sees that the integrand in Eq. (28),

$$Q = \cos\Theta_i\cos\Theta_k\delta[\sin\Theta_\diamond(\varepsilon)-|tr|(\sin\Theta_x+\sin\Theta_y)], \tag{30}$$

is a 2π-periodic function of Θ_x and Θ_y, provided they are considered as free variables, which allows us to expand the the integrand in the double-Fourier series:

$$Q_{ik} = \sum_{l_1=-\infty}^{\infty}\sum_{l_2=-\infty}^{\infty}A^{ik}_{l_1l_2}e^{i(l_1\Theta_x+l_2\Theta_y)}. \tag{31}$$

Since $\varepsilon_F/\hbar\omega_H \gg 1$, the exponents are fast-oscillating functions of P_x and P_y and, hence, the main contribution to the integral in Eq. (28) comes from the Fourier factor with $l_1 = l_2 = 0$, and therefore the sought integrand is approximately

$$Q_{ik}\approx A^{ik}_{00} = \frac{1}{(2\pi)^2}\int_{-\pi}^{\pi}d\varphi_x\int_0^{2\pi}d\varphi_y\cos\varphi_i\cos\varphi_k\delta[\sin\Theta_\diamond(\varepsilon)-|tr|(\sin\varphi_x+\sin\varphi_y)]. \tag{32}$$

Inserting Q_{ik} in the integral in Eq. (28), one finds the conductivity in the form

$$\sigma_{ik} = -2e^2t_0\frac{\bar{b}_i\bar{b}_k|tr|^2}{\pi mb_H^2}\frac{b_xb_y}{(2\pi\hbar)^2}\int d\varepsilon\frac{\partial f_0/\partial\varepsilon}{|\cos\Theta_\diamond|}\int_{-\pi}^{\pi}\int_{-\pi}^{\pi}d\varphi_xd\varphi_y\sin\varphi_i\sin\varphi_k\,\delta[\sin\Theta_\diamond(\varepsilon)-|tr|(\cos\varphi_x+\cos\varphi_y)], \tag{33}$$

where, while writing this expression, we shifted the integration variables $\varphi_{x,y}\to\varphi_{x,y}+\pi/2$ and, hence, the limits of integration to explicitly match the integral to the symmetry of the system. Using the symmetric properties of the integral and integrating the delta function, we obtain components of the magnetoconductivity tensor:

$$\sigma_{xx} = -e^2t_0\frac{b_y^2}{\pi^4m\hbar^2}\left[\frac{1}{2\pi}\left(\frac{b_xb_y}{2b_H^2}\right)\right]\int d\varepsilon\frac{\partial f_0/\partial\varepsilon}{|\cos\Theta_\diamond|}\int_{-\pi}^{+\pi}d\varphi\sqrt{|tr|^2-(|tr|\cos\varphi-\sin\Theta_\diamond(\varepsilon))^2}\,\boldsymbol{\Theta}[|tr|^2-(|tr|\cos\varphi-\sin\Theta_\diamond(\varepsilon))^2],$$
$$\sigma_{xy} = 0, \tag{34}$$

where $\boldsymbol{\Theta}$ is the Heaviside unit-step function, while the other two components, σ_{yy} and σ_{yx}, are simply obtained from the above expression by changing the indices $x\leftrightarrow y$. One should note the factor appearing in the square brackets multiplying the integral, which equals the integer number determined by the condition Eq. (15): it is proportional to $1/H$ (through b_H^2) that appears in the discrete quantities. Therefore, the obtained equation for the conductivity tensor, Eqs. (34), is valid at discrete values of the magnetic field H_l determined by Eq. (15). From the latter equation and Eqs. (34), one easily

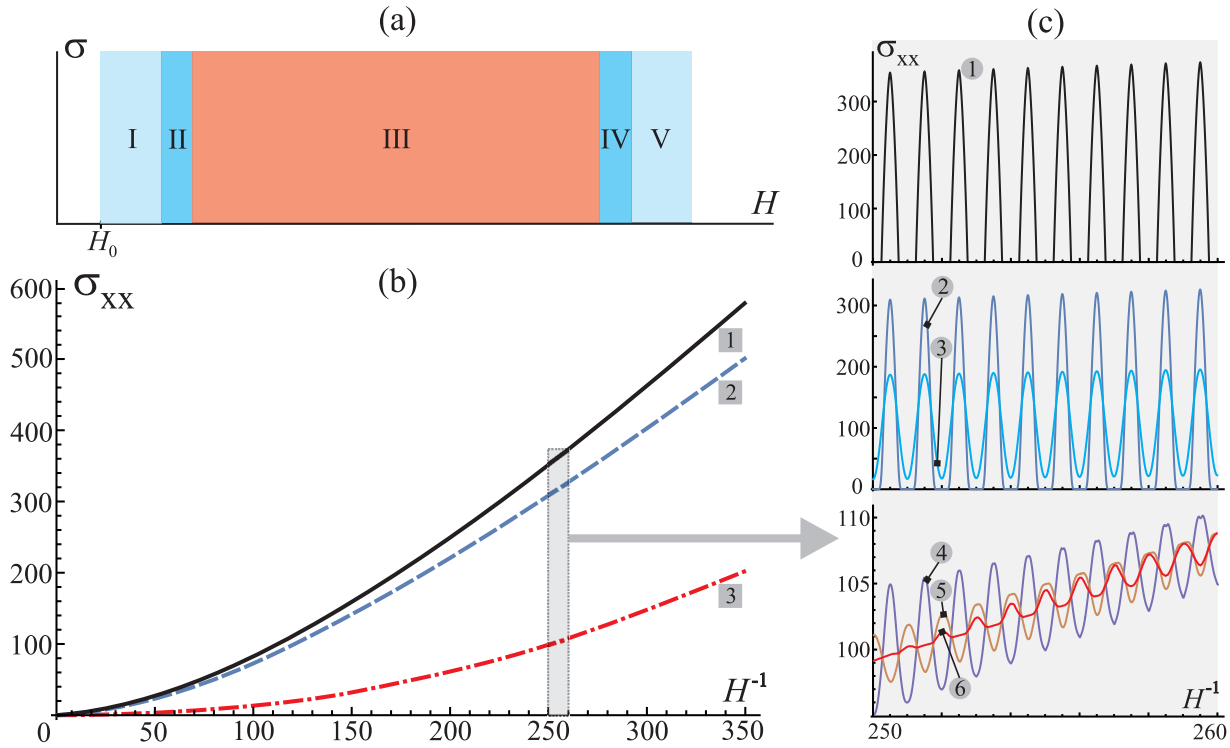

FIG. 3. (a) Characteristic intervals of magnetic field with qualitatively different behavior of magnetoconductivity with respect to development of the MB. H_0 is the lower limit of magnetic field in our consideration, for which $t_0\omega_{H_0} \gg 1$ holds (t_0 is the quasiparticle mean-free path time). In regions I and V, we have either small or large magnetic field for which $|r| \to 0$, or $|t| \to 0$, so the quasiparticles move along diamond-shaped or circular closed orbits, respectively. The magnetoconductivity attains the standard textbook form for closed holelike or electronlike orbits, i.e., Eq. (35) or (36), respectively. In region III, $|t|$ and $|r|$ are comparable, magnetoconductivity is given by Eqs. (34), and depicted in panels (b) and (c), here scaled by the factor multiplying the integral in Eqs. (34), proportional to H^{-1} through b_H^2, which has dimension of the 2D conductivity. II and IV are the crossover regions between the regimes described above. (b) An envelope (upper) of the oscillatory part of the longitudinal magnetoconductivity in region III versus inverse magnetic field (expressed in $\varepsilon_F/\hbar\omega_H$ dimensionelss units), depending on temperature: $k_BT/\varepsilon_F = 0$; 0.0001; 0.01 for curves 1–3, respectively. (c) An inset from panel (b), showing the oscillations of longitudinal magnetoconductivity versus inverse magnetic field (expressed in $\varepsilon_F/\hbar\omega_H$ dimensionelss units), depending on temperature: $k_BT/\varepsilon_F = 0$; 0.0001; 0.0005; 0.001; 0.005; 0.01 for curves 1–5, respectively.

finds that the distance between the neighboring points $H_l^{-1} - H_{l+1}^{-1}$ and the period of conductance oscillations, ΔH^{-1}, are incommensurate. From here it follows that the points H_l^{-1} gathered inside one period of the conductance oscillations cover it everywhere densely and, hence, Eqs. (34) present the conductivity tensor with very fine resolution. This result is valid in the limit of (magnetic) bandwidth significantly larger than the energy uncertainty related to quasiparticle scattering on impurities, i.e., $W \gg \hbar\nu_0$. It is depicted in Fig. 3 and is relevant for interval of magnetic fields marked by III in Fig. 3(a), where the characteristic intervals of magnetic field with qualitatively different behavior of magnetoconductivity with respect to the MB development are explained; for the sake of simplicity, the phase in the integral in Eqs. (29) and (34) is taken $\chi = \pi/4$.

There are several important points to notice regarding the result Eqs. (34). First, a remarkable fact is that the Hall effect is absent, i.e., $\sigma_{xy} = \sigma_{yx} = 0$. It is easy to obtain that result simply from the symmetry of the integral Eq. (33) by changing $\varphi_i \to -\varphi_i$. It happens in a wide range of magnetic fields in which the MB gives comparable probabilities $|t|^2$ and $|r|^2$ for motion along the closed orbits and tunneling between them. This means that the quasiparticle is delocalized in both directions of the 2D net, by the MB, performing motion as if there is effectively no magnetic field acting on it. Below we show that the Hall effect restores in the limits of relatively weak and relatively strong magnetic fields when quasiparticles move along the closed semiclassical trajectories.

The diagonal magnetoconductivity exhibits oscillations under a change of magnetic field—Fig. 3(b) shows the envelope, while the inset drawn in Fig. 3(c) shows the oscillations. As one can see from Eqs. (34) and Fig. 3, the period of oscillations is close to the period of the conventional de Haas-van Alphen or Subnikov-de Haas oscillations, but their amplitude is giant, becoming less pronounced with increasing temperature as well as changing the phase (due to integration of components with more periods depending on energy in the k_BT-window around the Fermi energy).

B. Magnetoconductivity in the limit of narrow bandwidth

As noted above, if the MB probability amplitudes are such that the inequality $W \ll \hbar\nu_0 \ll \hbar\omega_H$ is fulfilled, i.e., when the (magnetic) bandwidth is the smallest parameter, the quasiparticle band structure is a set of Landau levels slightly broadened

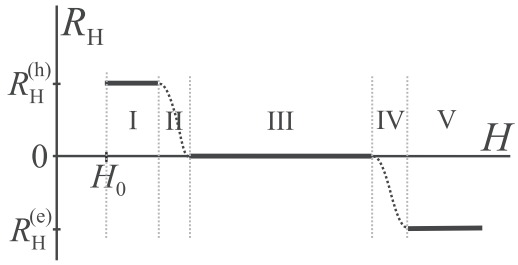

FIG. 4. Dependence of the Hall coefficient R_H on magnetic field (through the MB probability amplitude $|t(H)|$). In respectively weak magnetic field (still greater than H_0 for which $t_0\omega_{H_0} \gg 1$) —interval I, as well as in strong enough fields—interval V, such that the quasiparticle bandwidths are negligible, i.e., $W \ll \hbar\nu_0 \ll \hbar\omega_H$, the quasiparticles move along the diamond-shaped (hole) and circular (electron) trajectories, respectively. Consequently, the Hall coefficient is given by Eq. (38) or (41), respectively. In the wide intermediate magnetic field range in which $W \gg \hbar\nu_0$ (interval III), the quasiparticles freely move in both x and y directions, resulting in $R_H = 0$ due to the reciprocal lattice symmetry. Intervals II and IV are the crossover regions between the above-mentioned ones.

by the MB tunneling between the closed orbits. In this limit, we neglect that level broadening, i.e., we consider quasiparticles moving semiclassically along either the diamond-shaped orbit (rather weak magnetic fields, $|r| \ll 1$) or along the circular orbits (strong magnetic fields, $|t| \ll 1$) shown in Fig. 1. As a result, the magnetoconductivity tensor is the conventional one [23], that is,

(a) $|t| \to 1$ for the holelike trajectories

$$\sigma_{xx}^{(h)} = \sigma_{yy}^{(h)} = \frac{\sigma_0^{(h)}}{(t_0\omega_H)^2},$$
$$\sigma_{xy}^{(h)} = -\sigma_{yx}^{(h)} = \frac{n^{(h)}e}{H}, \tag{35}$$

(b) $|t| \to 0$ for the electronlike trajectories

$$\sigma_{xx}^{(e)} = \sigma_{yy}^{(e)} = \frac{\sigma_0^{(e)}}{(t_0\omega_H)^2},$$
$$\sigma_{xy}^{(e)} = -\sigma_{yx}^{(e)} = -\frac{n^{(e)}e}{H}, \tag{36}$$

where $\sigma_0^{(e,h)} = n^{(e,h)}e^2t_0/m$ is the conductivity of electrons (e), or holes (h) in the absence of magnetic field, while $n^{(e)} = \pi p_F^2/(2\pi\hbar)^2$ is the concentration of electrons and $n^{(h)} = [b^2 - \pi p_F^2]/(2\pi\hbar)^2$ concentration of holes. Here, for the sake of simplicity, we consider $b_x = b_y \equiv b$ and equal effective masses of electrons and holes, i.e., $m_e = m_h \equiv m$.

C. The Hall coefficient

Behavior of the Hall coefficient,

$$R_H \equiv \frac{E_y}{j_xH} = \frac{\sigma_{xy}}{(\sigma_{xx}\sigma_{yy} + \sigma_{xy}^2)H}, \tag{37}$$

with a change of magnetic field in the system under consideration is particularly remarkable as can be seen from Fig. 4.

In relatively weak magnetic fields, $|r(H)| \ll \nu_0/\omega_H \ll 1$, the MB is negligible, quasiparticles (holes) move along the diamond-shaped orbits (see Fig. 1) and hence the Hall coefficient

$$R_H \approx \frac{1}{en^{(h)}} \tag{38}$$

is positive (one should bear in mind that in all our expressions, e denotes the absolute value of electron charge).

After that, an increase of magnetic field results in an increase of the MB amplitude $|r(H)|$ to become comparable to $|t(H)|$ and (still in the limit $t_0\hbar\omega_H \gg 1$) the Hall coefficient is

$$R_H = 0. \tag{39}$$

The equality Eq. (39) is based on the symmetry of the MB net. Indeed, changing the integral variables in Eq. (28),

$$P_x = P_x' + \frac{b_H^2}{b_y}(\pi/2 - \mu + \nu),$$
$$P_y = P_x' - \frac{b_H^2}{b_y}(\pi/2 + \mu + \nu), \tag{40}$$

together with a change $P_x \to -P_x$ (or $P_y \to -P_y$), one obtains Eq.(39).

The Hall coefficient vanishes in the whole interval of magnetic fields for which $W \gg \hbar\nu_0$, as the quasiparticle is effectively delocalized in both directions of the 2D MB net.

With further increase of magnetic field, in the limit $|t(H)| \ll \nu_0/\omega_H \ll 1$, the Hall coefficient restores to nonvanishing value, changing its sign from positive to negative because the quasiparticles move along the electronlike circular orbits in this limit, i.e.,

$$R_H \approx -\frac{1}{en^{(e)}}. \tag{41}$$

IV. CONCLUSION

Quantum dynamics and kinetics of quasiparticles, under strong magnetic field, in the 2D net of diamond-shaped semiclassical trajectories, generated by the reconstruction of initially circular FS by the biaxial DW, coupled by the MB are considered. We present an analytical solution of the 2D MB problem, within the semiclassical approximation. We find that the obtained quasiparticle spectrum and wave functions of Bloch type, in the momentum representation, are functions of the conserved 2D generalized momentum $\mathbf{P} = (P_x, P_y)$ if magnetic field satisfies the rational magnetic flux quantization rule analogous to the Zak/Hofstdater condition. The quasiparticle spectrum is found to be the series of alternating 2D energy bands of the width proportional to the magnetic energy $\hbar\omega_H$, and gaps between them, both in detail determined by the MB amplitude of the quasiparticle tunneling between the semiclassical trajectories.

Using the explicit expression for the dispersion equation, we find that the diagonal magnetoconductivity σ_{xx} and σ_{yy} oscillate with a giant amplitude when magnetic field is changed. Period of these oscillations with respect to the inverse magnetic field is proportional to the area of the pocket in the momentum space encircled by the semiclassical quasiparticle trajectory. We also show that the nondiagonal conductivity is equal to zero, i.e., $\sigma_{xy} = \sigma_{yx} = 0$ in a wide range of magnetic fields in which the width of the quasiparticle band is much

larger than the energy uncertainty caused by the quasiparticle-impurity scattering, and in which the MB probabilities for a quasiparticle to move along the semiclassical trajectories and to tunnel between them are comparable. In such conditions, the quasiparticle moves freely in x and y directions in the 2D net as if there is effectively no magnetic field acting on it to cause the Hall effect, consequently resulting in vanishing Hall coefficient.

In the opposite limit of negligibly narrow bandwidth with respect to the impurity scattering energy uncertainty, the spectrum is a set of discrete Landau levels and the magnetoconductivity tensor is the conventional one for closed trajectories, well-known from textbooks. For relatively weak fields, when small MB tunneling probability yields the preferable motion along the closed diamond-shaped hole orbits, we have a standard expression for the Hall coefficient, inversely proportional to concentration of carriers (holes), with positive sign. On the other hand, for relatively strong magnetic fields, when strong MB tunneling probability between hole orbits reconstructs the preferable motion of carriers along the closed electronlike circular orbits, we again have the standard expression for the Hall coefficient, inversely proportional to concentration of carriers (electrons) but now with negative sign. Altogether, we have the holelike Hall effect for weak field, switching to the electronlike one for strong fields, with wide intervals of magnetic field with vanishing Hall effect between them. Our preliminary estimations show that the analytical magnetoconductivity model suggested here may be used to explain the absence of the Hall effect and change of its sign observed in certain experiments in high-T_c superconducting cuprates [10,11].

ACKNOWLEDGMENTS

This work was supported by the Croatian Science Foundation, Project No. IP-2016-06-2289, and by the QuantiXLie Centre of Excellence, a project cofinanced by the Croatian Government and European Union through the European Regional Development Fund—the Competitiveness and Cohesion Operational Programme (Grant No. KK.01.1.1.01.0004).

APPENDIX A: GENERAL FORMULA FOR CURRENT OF DELOCALIZED QUASIPARTICLES

Introducing the symmetric operator of electron density at a point $\mathbf{R}$ in the coordinate space,

$$\hat{n}(\mathbf{R}) = \tfrac{1}{2}[\hat{\rho}\delta(\hat{\mathbf{r}} - \mathbf{R}) + \delta(\hat{\mathbf{r}} - \mathbf{R})\hat{\rho}], \tag{A1}$$

one writes the local current density at the point $\mathbf{R} = (X, Y)$ in the form

$$\mathbf{j}(\mathbf{R}) = -2e\mathrm{Tr}(\hat{\mathbf{v}}\hat{n}(\mathbf{R})), \tag{A2}$$

factor 2 coming from the quasiparticle spin.

Writing the trace in the representation of the proper functions of Hamiltonian $\hat{H}_0$ and using Eq. (24), one finds the current density

$$j_i(\mathbf{R}) = -2e^2 t_0 \sum_{\kappa} E_k \frac{\partial \varepsilon_\kappa}{\partial P_k}\frac{\partial \varepsilon_\kappa}{\partial P_i}\frac{\partial f_0}{\partial \varepsilon_\kappa}\varphi^\star_\kappa(\mathbf{R})\varphi_\kappa(\mathbf{R}), \tag{A3}$$

where $\mathbf{E}$ is electric field and $i \in \{x, y\}$. Here φ_κ is the electron proper Bloch functions

$$\varphi_{n,\mathbf{P}}(\mathbf{R}) = e^{i\mathbf{P}\mathbf{R}/\hbar}u_{n,\mathbf{P}}(\mathbf{R}) \tag{A4}$$

in the coordinate representation, $\kappa = (n, \mathbf{P})$, i.e., the band index and conserved generalized momentum, respectively. The total current flowing along the plate of the length L_x and the width L_y is

$$\mathbf{I} = \int_{-L_x/2}^{L_x/2} dX \int_{-L_y/2}^{L_y/2} dY\ \mathbf{j}(\mathbf{R}). \tag{A5}$$

Using the normalization condition for the periodic factors in Bloch functions, one finds

$$\int_{-L_x/2}^{L_x/2} dX \int_{-L_y/2}^{L_y/2} dY u^\star_{n,\mathbf{P}}(\mathbf{R})u_{n,\mathbf{P}}(\mathbf{R}) = L_X L_Y \tag{A6}$$

and, hence, the current density averaged over the sample, $\mathbf{J} = \mathbf{I}/L_x L_y$, is

$$J_i = -2e^2 t_0 \sum_n E_k \int \frac{d\mathbf{P}}{(2\pi\hbar)^2}\frac{\partial \varepsilon_n}{\partial P_i}\frac{\partial \varepsilon_n}{\partial P_k}\frac{\partial f_0}{\partial \varepsilon}\Big|_{\varepsilon=\varepsilon_n(\mathbf{P})}. \tag{A7}$$

APPENDIX B: CALCULATION OF CURRENT IN TERMS OF DISPERSION FUNCTION

Solution of the dispersion equation Eq. (18) appearing in Eq. (26) is $\varepsilon = \varepsilon_n(\mathbf{P})$, thus the dependence of v_i on $\mathbf{P}$ is $v_i(\mathbf{P}) = v_i(\varepsilon_n(\mathbf{P}), \mathbf{P})$. The latter dependence allows us to rewrite Eq. (25) in the form

$$\sigma_{ik} = -2e^2 t_0 \int \frac{d\mathbf{P}}{(2\pi\hbar)^2}\int d\varepsilon \frac{\partial f_0}{\partial \varepsilon} v_i(\varepsilon, \mathbf{P})v_k(\varepsilon, \mathbf{P}) \times \sum_n \delta[\varepsilon - \varepsilon_n(\mathbf{P})]. \tag{B1}$$

Using the known mathematical identity

$$\delta[f(x)] = \sum_k \frac{\delta[x - x_k]}{f'(x)}, \tag{B2}$$

where x_k are zeros of function $f(x)$, and Eq. (26), one finds Eq. (27) from the main text.

[1] G. Grüner, Rev. Mod. Phys. **60**, 1129 (1988).
[2] R. E. Peierls, Ann. Phys. **4**, 121 (1930).
[3] J. P. Pouget, Semicond. Semimet. **27**, 87 (1988); Crystals **2**, 466 (2012).

[4] R. E. Thorne, Phys. Today **49**(5), 42 (1996).
[5] B. Keimer, S. A. Kivelson, M. R. Norman, S. Uchida, and J. Zaanen, Nature (London) **518**, 179 (2015).
[6] K. C. Rahnejat, C. A. Howard, N. E. Shuttleworth, S. R. Schofield, K. Iwaya, C. F. Hirjibehedin, Ch. Renner, G. Aeppli, and M. Ellerby, Nat. Commun. **2**, 558 (2011); R. Shimizu, K. Sugawara, K. Kanetani, K. Iwaya, T. Sato, T. Takahashi, and T. Hitosugi, Phys. Rev. Lett. **114**, 146103 (2015).
[7] A. M. Kadigrobov, A. Bjeliš, and D. Radić, Phys. Rev. B **97**, 235439 (2018).
[8] A. M. Kadigrobov, D. Radić, and A. Bjeliš, Phys. Rev. B **100**, 115108 (2019).
[9] M. Spaić and D. Radić, Phys. Rev. B **103**, 075133 (2021).
[10] D. LeBoeuf, N. Doiron-Leyraud, J. Levallois, R. Daou, J.-B. Bonnemaison, N. E. Hussey, L. Balicas, B. J. Ramshaw, R. Liang, D. A. Bonn, W. N. Hardy, S. Adachi, C. Proust, and L. Taillefer, Nature (London) **450**, 533 (2007); S. Badoux, W. Tabis, F. Laliberté, G. Grissonnanche, B. Vignolle, D. Vignolles *et al. ibid.* **531**, 210 (2016).
[11] Z. Shi, P. G. Baity, J. Terzic, B. K. Pokharel, T. Sasagawa, and D. Popović, Nat. Commun. **12**, 3724 (2021).
[12] Topological reconstruction of closed FSs into a 1D chain of FSs was suggested and its stability investigated in our recent papers [7–9].
[13] A. M. Kadigrobov, A. Bjeliš, and D. Radić, Eur. Phys. J. B **86**, 276 (2013).
[14] A. M. Kadigrobov, D. Radić, and A. Bjeliš, Phys. B: Condens. Matter **480**, 248 (2015).
[15] A. M. Kadigrobov, A. A. Slutskin, and S. A. Vorontsov, J. Phys. Chem. Solids **53**, 387 (1992).
[16] J.-Y. Fortin and A. Audouard, Low. Temp. Phys. **43**, 173 (2017).
[17] E. I. Blount, Phys. Rev. **126**, 1636 (1962).
[18] A. A. Slutskin and A. M. Kadigrobov, Fiz. Tverd. Tela (Leningrad) **9**, 184 (1967) [Sov. Phys. Solid State **9**, 138 (1967)].
[19] A. A. Slutskin, Zh. Eksp. Teor. Fiz. **53**, 676 (1967) [Sov. Phys. JETP **26**, 474 (1968)].
[20] Experimental study of the magnetoresistance in 2D network of quasiparticle orbits coupled by the magnetic breakdown is reported in the paper A. Audouard, D. Vignolles, I. Sheikin, R. B. Lyubovskii, and R. N. Lyubovskaya, Europhys. Lett. **71**, 783 (2005).
[21] J. Zak, Phys. Rev. **134**, A1602 (1964); **134**, A1607 (1964).
[22] D. R. Hofstadter, Phys. Rev. B **14**, 2239 (1976).
[23] I. M. Lifshits, M. Ya. Azbel, and M. I. Kaganov, *Electron Theory of Metals* (Consultants Bureau (Plenum), New York, 1973).
[24] I. M. Lifshitz and A. M. Kosevich, Zh. Eksp. Teor. Fiz. **29**, 730 (1955) [Sov. Phys. JETP **2**, 636 (1956)].
[25] L. Onsager, Philos. Mag. **43**, 1006 (1952).
[26] M. H. Cohen and L. M. Falicov, Phys. Rev. Lett. **7**, 231 (1961).
[27] If the magnetic field corresponds to the case that the Hamiltonian commutes with the operator of translation on nb_x and b_y (here $n \geqslant 1$), the term $2\pi l$ on the right-hand side of Eq. (15) is changed to $2\pi l/n$ and hence the flux ratio is $\Phi_0/\Phi = p/q$ with p and q integers for all rational magnetic fields.
[28] J. Solyom, *Fundamentals of the Physics of Solids* (Springer-Verlag, Berlin, 2010), Vol. II, Chap. 22.3.4.
[29] M. I. Kaganov and A. A. Slutskin, Phys. Rep. **98**, 189 (1983).